CRYSTAL GROWTH & DESIGN

Systematics in NH$^+\cdots$N-Bonded Monosalts of 4,4′-Bipyridine (44′biPy) with Mineral Acids

Małgorzata Ratajczak-Sitarz, Andrzej Katrusiak,* Zofia Dega-Szafran, and Grzegorz Stefański

Faculty of Chemistry, Adam Mickiewicz University, Umultowska 89b, 61-614 Poznań

Supporting Information

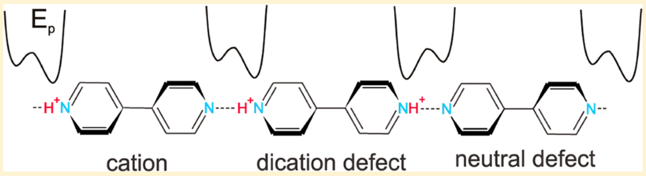

ABSTRACT: Despite significantly different crystal symmetry and packing, the crystal structures of NH$^+\cdots$N hydrogen-bonded salts of 4,4′-bipyridine (44′biPy) with mineral acids *HA* = HCl, HBr, HI, HClO$_4$, HBF$_4$ and H$_2$SiF$_6$ exhibit close analogies in the hydration, aggregation of the cations and their twisted conformation, as well as proton disordering. All monosalts have been synthesized and, at normal conditions, form crystals of general formula $[44'\mathrm{biPyH}]^+A^-\cdot x\mathrm{H_2O}$ (x = 0.5, 1, or 2), and $[44'\mathrm{biPyH}]^+{}_2\mathrm{SiF_6}^{2-}\cdot 5\mathrm{H_2O}$. In the structures, the 44′biPyH$^+$ cations are NH$^+\cdots$N bonded into linear chains, and in most $[44'\mathrm{biPyH}]^+A^-\cdot x\mathrm{H_2O}$ crystals the protons are disordered, similarly as in anisotropic relaxors 1,4-diazabicyclo[2.2.2]octane hydroiodide and hydrobromide (dabcoHI and dabcoHBr, respectively). The proton disorder implies generation of point defects of neutral 44′biPy molecules and $[44'\mathrm{biPyH_2}]^{2+}$ dications in all these structures. In all $[44'\mathrm{biPyH}]^+A^-$ structures investigated, the acid anions are hydrogen bonded to water molecules and interact with pyridine hydrogen atoms. Two polymorphs of $[44'\mathrm{biPyH}]^+\mathrm{I}^-\cdot\mathrm{H_2O}$ differ in color: the orthorhombic polymorph α is yellow, and the triclinic polymorph β is orange.

1. INTRODUCTION

Fast progress in electronics and miniaturization of electronic devices in the last decades stimulates the search for new dielectric materials with refined properties. For example, miniature capacitors applied in commonly used devices, such as portable memories, cell phones, and computers, require insulators with increased electric permittivity (ε). The most efficient materials of this type currently in use belong to the group of composites or ceramic ferroelectric relaxors that are based on mixed perovskite structures.[1] The currently used perovskite ceramics are expensive in processing and doped with lead, posing the threat of environmental contamination. Therefore, cheaper and environmentally friendly ferroelectric and relaxor materials are intensively sought.[1] The required ferroelectric behavior was reported for the monosalts of 1,4-diazabicyclo[2,2,2]octane (dabco, C$_6$H$_{12}$N$_2$) with mineral acids.[2,3] It was found that dabco hydroiodide exhibits a uniaxial giant relaxor response, with the dielectric constant exceeding 4000 along [001].[4,5] In the structure of dabco monosalts, dabcoH$^+$ cations aggregate into chains linked by medium-strength directional homoconjugated NH$^+\cdots$N hydrogen bonds.[6] The short-range spontaneous polarization of the dabco chains is the main cause of the existence of relaxor behavior in this kind of compounds. Much weaker effects were detected in dabco tetrafluoroborate (dabcoHBF$_4$) and in salts of pyrazine.[7] Thus far, the giant dielectric response was found in hexagonsl dabco*HA* crystals with spherical anions (*A* = Br$^-$, I$^-$).[8]

It was established that the ferroelectric relaxor properties in dabcoHI and dabcoHBr are generated by highly polarizable NH$^+\cdots$N bonds. For a better understanding of their structure-property relation we have undertaken this systematic study of the monosalts of the 4,4′-bipyridine (44′biPy, Scheme 1) with mineral acids *HA*: HCl, HBr, HI, HClO$_4$, and HBF$_4$; abbreviation 44′biPy*HA* denotes the monosalts, which form NH$^+\cdots$N-bonded aggregates similar to those in dabco*HA*. The study included an analogous salt built of 4-pyridine-4′-pyridinium cations 44′biPyH$^+$ and divalent SiF$_6{}^{2-}$ anions. Some salts of the mono- (1:1) and diprotonated (1:2) 44′biPy with mineral acids were synthesized, and their IR spectra were studied earlier.[9] The structure of several disalts of 44′biPy were determined till now (for example, 44′biPy2HI,[10] 44′biPy2HCl,[11] 44′biPy2HNO$_3$,[11] 44′biPy2HClO$_4$[12]). However, our study has been focused on 44′biPy*HA* monosalts, as they are likely to resemble the NH$^+\cdots$N-bonding pattern in dabco*HA* salts and their ferroelectric and relaxor properties. Moreover, the H disordering in NH$^+\cdots$N-bonded monosalts generates neutral and dicationic defects, 44′biPy and

Scheme 1. Atomic Labels in the 4,4′-Bipyridinium Cation[a]

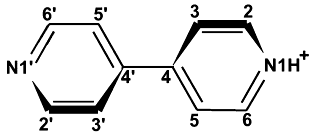

[a] Protons have been labeled according to their carriers.

Received: May 15, 2013
Revised: August 1, 2013
Published: August 6, 2013

Table 1. Crystal Data and Experimental Details of the 4,4′-Bipyridinium Monosalts with Mineral Acids HBr, HCl, HI, $HClO_4$, HBF_4, and H_2SiF_6, all at 296 K[a]

compound	44′biPyHBr $\cdot H_2O$	44′biPyHCl $\cdot 2H_2O$	α-44′biPyHI $\cdot H_2O$	β-44′biPyHI $\cdot H_2O$	44′biPy$HClO_4$ $\cdot 2H_2O$	44′biPyHBF_4 $\cdot {}^1/_2H_2O$	44′biPy$_2H_2SiF_6$ $\cdot 5H_2O$
chemical formula	$[C_{10}H_9N_2]^+Br^-$ $\cdot H_2O$	$[C_{10}H_9N_2]^+Cl^-$ $\cdot 2H_2O$	$[C_{10}H_9N_2]^+I^-$ $\cdot H_2O$	$[C_{10}H_9N_2]^+I^-$ $\cdot H_2O$	$[C_{10}H_9N_2]^+ClO_4^-$ $\cdot 2H_2O$	$[C_{10}H_9N_2]^+BF_4^-$ $\cdot {}^1/_2H_2O$	$[C_{10}H_9N_2]^+_2SiF_6^{2-}$ $\cdot 5H_2O$
color	colorless	colorless	yellow	orange	colorless	colorless	colorless
cryst syst	orthorhombic	orthorhombic	orthorhombic	triclinic	triclinic	monoclinic	orthorhombic
space group	$P2_12_12_1$	$Pnma$	$P2_12_12_1$	$P\bar{1}$	$P\bar{1}$	$C2/c$	$Pnc2$
a (Å)	7.1899(2)	9.7364(3)	7.4178(2)	8.0716(3)	8.1537(7)	17.834(3)	9.7617(14)
b (Å)	9.6920(3)	7.2529(4)	9.7087(2)	8.8465(3)	9.765(2)	7.968(1)	7.235(2)
c (Å)	15.3562(4)	15.8123(6)	15.9239(4)	9.7150(3)	17.709(2)	16.625(3)	17.101(3)
α (deg)	90	90	90	93.471(3)	78.14(3)	90	90
β (deg)	90	90	90	112.882(4)	82.87(3)	104.26(2)	90
γ (deg)	90	90	90	113.452(4)	67.43(3)	90	90
vol. (Å^3)	1070.09(5)	1116.62(8)	1146.79(5)	566.98(3)	1272.6(4)	2289.7(7)	1207.8(4)
Z/Z'	4/1	4/0.5	4/1	2/1	4/2	8/1	2/0.5
D_x (g/cm^3)	1.584	1.360	1.750	1.770	1.528	1.468	1.503
no. of unique reflns	2732	1587	2957	2808	5957	2524	3046
R_{int}	0.0170	0.0140	0.0160	0.0112	0.0302	0.0272	0.0176
goodness of fit (F^2)	1.003	1.005	0.980	1.060	1.007	1.016	1.065
final R_1 ($I > 2\sigma_I$)	0.0293	0.0550	0.0220	0.0260	0.0698	0.0589	0.0464
final R_2 ($I > 2\sigma_I$)	0.0854	0.2050	0.0490	0.0667	0.2040	0.1492	0.1366

[a] Two polymorphs of the hydroiodide are labeled α and β.

44′biPyH_2^{2+}, respectively. These defects can considerably affect the properties of these crystals. The only known structures of monoprotonated 44′biPy salts are hydrobromide monohydrate[13] and hydroperchlorate dihydrate.[14] However, their dielectric properties in relation to the protons dynamics were not considered. Therefore, we determined the dimensions and possible transformations of their $NH^+\cdots N$ bonds at normal conditions. We found that the 44′biPyH*A* salts form preferably hydrates, which is disadvantageous for their possible applications; therefore, their dielectric properties have not been pursued in this study. Another interesting aspect of the H-bonded salts of 44′biPy is its conformation, as 44′biPy is often used as a building block (linker) of organic and metal-organic zeolites, forming covalent organic frameworks (COF) and metal-organic frameworks (MOF).

2. EXPERIMENTAL SECTION

Syntheses of the 4,4′-bipyridinium:H*A* Salts. 4,4′-Bipyridine salts with mineral acid at the stoichiometry 44′biPy:H*A* = 1:2 and 1:1 were prepared according methods described earlier.[9] The disalts, 44′biPy2H*A*, were prepared by adding a small excess of acid to the diethyl ether solution of 44′biPy. The precipitate after recrystallization could be easily characterized by the melting point: 44′biPy2HBr·H_2O at 302−303 °C, 44′biPy2HCl at 228 °C, 44′biPy2HI at 308−312 °C, 44′biPy2$HClO_4$ at 324 °C, 44′biPy2HBF_4 at 222−224 °C. These disalts were each mixed with an equimolar amount of 44′biPy, leading to the monosalts, 44′biPyH*A* obtained in the form of hydrates. Their melting points are 44′biPyHBr·H_2O 256 °C, 44′biPyHCl·2H_2O 233 °C, α-44′biPyHI·H_2O 312−313 °C, β-44′biPyHI·H_2O 296 °C, 44′biPy$HClO_4$·2H_2O 318−319 °C, and 44′biPyHBF_4·1/2H_2O 179 °C (Table S1, Supporting Information). Salts of 44′biPyHI crystallized in two polymorphic forms, α and β. Details of the syntheses are described in the Supporting Information.

One of the crystals selected from the vial with 44′biPyHBF_4·1/2H_2O was found to be a salt containing the SiF_6^{2-} anion, 44′biPy$_2H_2SiF_6$·5H_2O. It was probably formed by the impurities in the HBF_4 acid used for syntheses of 44′biPyHBF_4 or resulted from interactions of HBF_4 with glass vials. In fact we noticed that the vial used for the synthesis and crystallization of 44′biPyHBF_6·H_2O had the inner surface eroded after the experiment. Because of its structure built of 44′biPyH^+ cations $NH^+\cdots N$ bonded into chains, we included this salt for comparison. A subsequent check of the vial contents confirmed that it contained 44′biPyHBF_4·1/2H_2O crystals only, and no other 44′biPy$_2H_2SiF_6$·5H_2O crystals could be found.

X-ray Diffraction Analyses. The 44′biPyH*A* salts were recrystallized from methanol in order to obtain samples suitable for single-crystal X-ray studies. A KUMA KM4-CCD diffractometer was used. Data reduction was performed with the CrysAlisPro and CrysAlisRed programs. Absorption of crystals was corrected analytically. Structures were solved by direct methods using the SHELXS-97 program and refined with full-matrix least-squares on reflections intensities (F^2) with SHELXL-97.[15] Structural drawings were prepared using programs XP and POV-ray.

Positions of pyridine H atoms have been calculated from the molecular geometry, and pyridinium protons have been located from difference Fourier (Δ*F*) maps. In all structures, except the 44′biPy$_2H_2SiF_6$·5H_2O hydrate, the Δ*F* maps contained peaks corresponding to the protons appearing at both N(1) and N(1′) atoms, indicating the disorder of protons. Therefore, for all the structures the model including the disorder and partial site occupation factors (SOFs) at both N atoms in the form SOF(N1) + SOF(N1′) = 1 was refined.

While solving the 44′biPyHCl·2H_2O structure, the cation atoms were initially located on the mirror plane perpendicular to [*y*]. However, all thermal ellipsoids of carbon atoms were strongly elongated along [*y*], so the carbon atoms and their hydrogens have been allowed to refine (with SOF's fixed to 0.5) off the mirror plane. This disordered model refined to considerably lower residue *R* factors. It was attempted to refine the structure in the reduced symmetry of space group $Pn2_1a$, but the disorder persisted despite the absence of a mirror plane, and the *Pnma* symmetry model has been retained (Table 1). In the final model the cation lies on a mirror plane, and the atomic positions of atoms N1, C4, C4′, and N1′ are ordered, while other atoms are split between two sites. The angles between the planes of disordered rings are 18.4(4)° and 19.6(4)°. It is also possible that the planar cation jumps between the two sites. In other monosalts investigated in this study the pyridine rings are ordered. In 44′biPyBF_4·1/2H_2O at 296 K the BF_4^- anion is disordered.

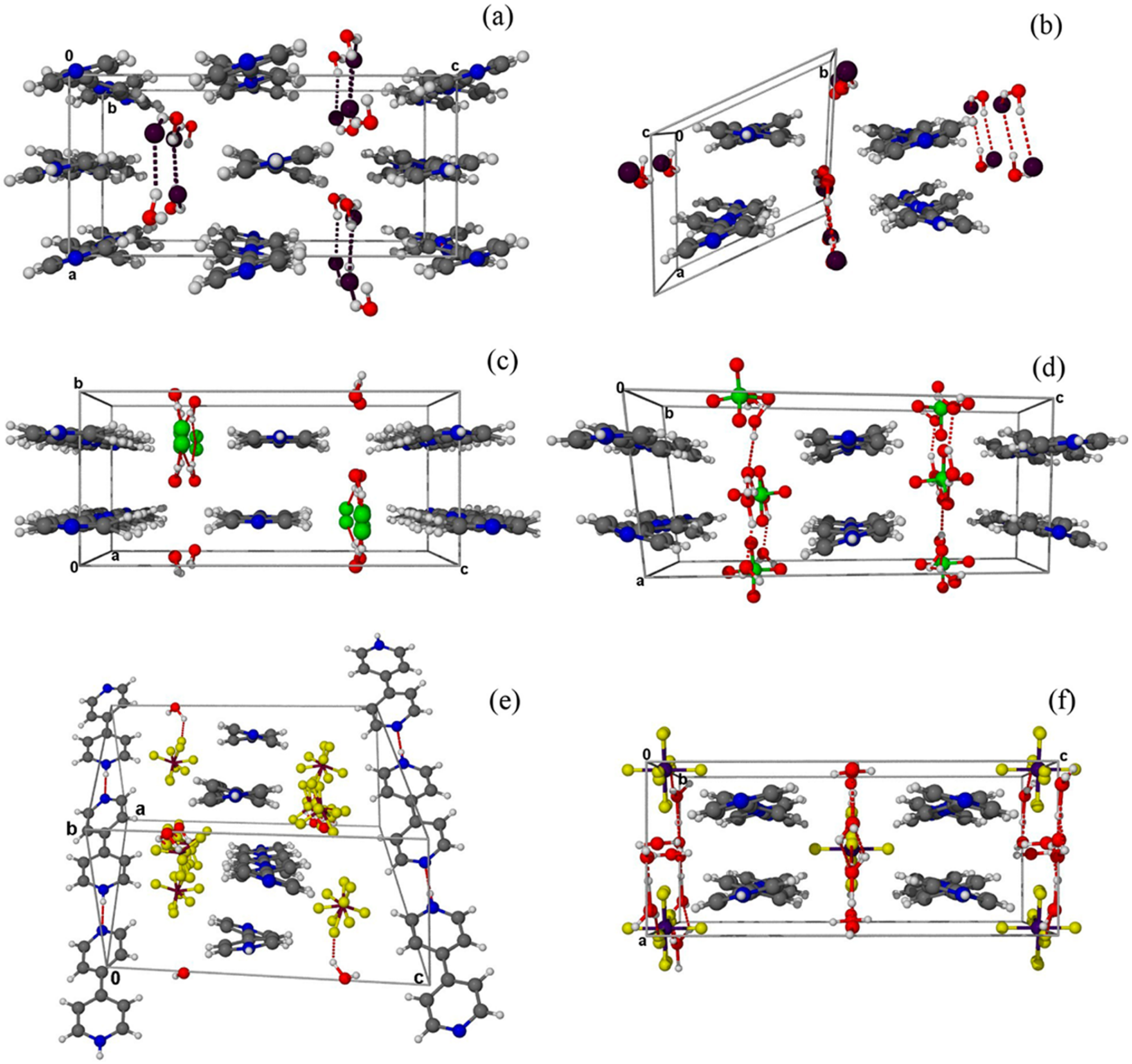

Figure 1. Crystal structures of (a) 44′biPyHI·H_2O polymorph *α*, isostructural with 44′biPyHBr·H_2O, (b) 44′biPyHI·H_2O polymorph *β*, (c) 44′biPyHCl·$2H_2O$, (d) 44′biPyHClO_4·$2H_2O$, (e) 44′biPyHBF_4·1/2H_2O, and (f) 44′$biPy_2H_2SiF_6$·$5H_2O$; all viewed along the bipyridinium NH^+···N-bonded chains. H bonds are shown as dotted lines. Disordered sites of 44′biPyH^+ are shown in (c) and BF_4^- in (e).

3. RESULTS AND DISCUSSION

The 44′biPyH*A* monosalts exhibit surprisingly close common features, despite different space-group symmetry, different arrangement of H-bonded aggregates, and even hydration stoichiometry 44′biPyH*A*·xH_2O ranging $1/2 \leq x \leq 2$ and different anion valence in 44′$biPy_2H_2SiF_6$ (Table 1). It is characteristic that in all investigated 44′biPyH*A* monosalts (i) the 44′biPyH^+ cations are NH^+···N bonded into linear chains, (ii) the cations do not display the internal crystallographic symmetry (except 44′biPyHCl·$2H_2O$, where the cation is disordered with half-occupied sites located off the mirror plane), (iii) the cations are in the twisted conformation, (iv) the anions are located between the chains and close to the region of NH^+···N bonds, (v) all monosalts are hydrates, and (vi) the protons are disordered at 296 K. Features (i) and (iv) also apply to all structures of dabcoH*A* salts. The considerable difference is the hydration of 44′biPyH*A* salts, which has not been observed in any dabcoH*A* structures at ambient pressure.[6] None of the dabcoH*A* salts, where *A* = Br, I, ClO_4, BF_4, and ReO_4, formed hydrates at normal conditions, but it was shown that pressure induces hydration of dabcoHI:[16] structures of two high-pressure dabcoHI·H_2O polymorphs were determined.

The NH^+···N-bonded linear chains of 4,4′-bipyridinium cations in the investigated structures are shown in Figures 1 and 2. The chains run along the [010] direction except for the 44′biPyHCl·$2H_2O$ crystal, where it runs down [100], and the 44′biPyHBF_4·1/2H_2O where the chains run down [110] and [$1\bar{1}0$] directions. Thus, in all the investigated 44′biPyH*A*·xH_2O structures the chains are parallel, except for 44′biPyHBF_4·1/2H_2O, where two sets of parallel chains form angle $\delta = 2\mathrm{tg}^{-1}(b/a) = 48.14°$ (*a* and *b* are the unit-cell dimensions, cf. Table 1). At 296 K, the protons are disordered in the hydrogen bonds in all investigated 44′biPyH*A*·xH_2O structures but the protons are ordered in 44′$biPy_2H_2SiF_6$·$5H_2O$. According to a recent study on dabcoHI polymorphs, the relaxor properties of dabcoHI phase V are generated by the local ordering of the protons in polar nanoregions and to the hexagonal symmetry of the average crystal structure.[8,17] The relaxor behavior is based

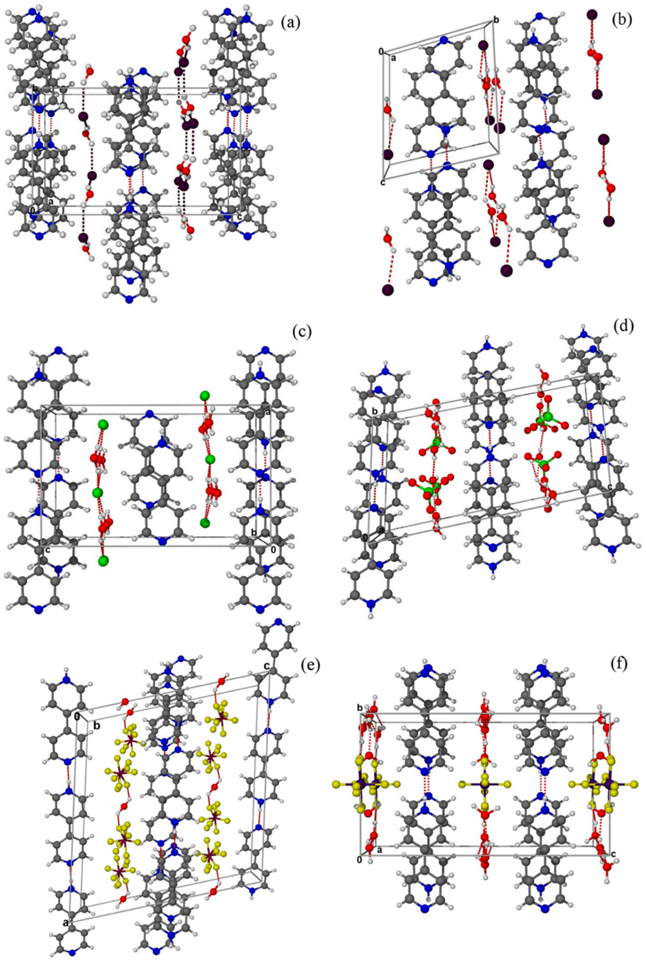

Figure 2. Structures of 44′biPyH*A* hydrates illustrating the NH^+···N-bonded bipyridinium chains: (a) 44′biPyHI·H_2O polymorph *α*, isostructural with 44′biPyHBr·H_2O, (b) 44′biPyHI·H_2O polymorph *β*, (c) 44′biPyHCl·$2H_2O$, (d) 44′biPyHClO$_4$·$2H_2O$, (e) 44′biPyHBF$_4$·1/2H_2O, and (f) 44′biPy$_2$H$_2$SiF$_6$·5H_2O. For clarity, only one of the disordered proton sites has been shown (cf. Figure 1).

on the polarization of the chains and local ordering of protons in nanodomains.[8,18]

The water molecules in all investigated 44′biPyH*A* monosalts form hydrogen bonds to the anions and form weak H bonds to the hydrogen atoms of the pyridine ring. The most common pattern between the water molecules and anions are hydrogen-bonded ···HOH···A^-··· chains running along the chains of NH^+···N-bonded cations. Such chains are present in *α*-44′biPyHI·H_2O and 44′biPyHBr·H_2O. The shortest distances between anions and cations are by about 0.2 Å longer than the sum of the atomic van der Waals radii.[19] This structural feature can be attributed to the water molecules, which dominate the hydrogen-bonding interaction involving the anions. The CH··· A^- contacts are present in dabcoH*A* salts, none of which contained crystalline water at ambient conditions.

The NH^+···N-bonded chains can be characterized by the length of their segments, consisting of one 44′biPyH$^+$ cation, the cation's conformation, mutual orientation of the neighboring cations, and the ordered or disordered proton location (Table 2). Temperature significantly affects the 44′biPyHBr·H_2O in this respect that at 90 K the proton becomes ordered but other H-bonded chain parameters remain hardly changed: the segment length *L* becomes 9.684(3) Å, and angles $\tau_1/\tau_2/\tau_3$ are 29.6(4)°/29.6(4)°/−35.2(4)°.[13] These parameters are similar for all 44′biPyH*A*·*x*H_2O structures investigated. On average, the chain segment *L* is about 9.74 Å long, and the shortest segment in 44′biPyHBr·H_2O is only 0.05 Å shorter. The 44′biPy conformation is between 18.3 and 36.5°. The disorder of pyridine rings in 44′biPyHCl·$2H_2O$ may be due to the effect of the crystal environment, consistent with the conjunction of aromatic rings through the C4−C4′ bond favoring the planar conformation and counteracted by the repulsion between the pyridine H atoms *ortho* to the C4−C4′ junction (at atoms C3, C5, C3′, and C5′). The classical example of the competition between the conjunction of aromatic rings and repulsion of their H atoms leads to phase transitions in biphenyl and higher polyphenyls.[20−26] In the biphenyl crystal at normal conditions the phenyl rings in molecules are parallel and the molecules are located at the inversion center. In all investigated 44′biPyH*A*·*x*H_2O salts, except 44′biPyHCl·$2H_2O$, the cations lie at general positions and there are no symmetry requirements restricting the torsion of rings about bond C4−C4′. Likewise, there are no restrictions concerning the proton site. Nonetheless, at 296 K protons are disordered in the 44′biPyH*A*·*x*H_2O salts at ratios between 89:11 and close to 50:50 (Table 2). This is similar to the disordered protons in cationic chains of dabcoHBr and dabcoHI, leading to high polarizability of NH^+···N bonds and anisotropic relaxor properties. These observations of the proton disorder are consistent with the effect of atomic displacements coupled to the H sites in hydrogen bonds.[27] In dabcoHBr and

Table 2. Parameters of NH^+···N′ Bonded Cationic Chains in 44′biPyH*A*·*x*H_2O and 44′biPy$_2$H$_2$SiF$_6$·5H_2O Hydrates at 296 K[a]

	chain directions	*L* [Å]	τ_1/τ_2 [deg]	τ_3 [deg]	SOF H1	η/η' [deg]
44′biPyHBr·H_2O	[010]	9.6920(3)	29.5(5)/29.6(5)	−35.3(4)	0.89(6)	174.3(2)/172.9(2)
44′biPyHCl·$2H_2O$	[100]	9.7364(3)	19.3(9)/18.3(9)	−20.5(9)	0.53(2)	179.5(1)/179.8(1)
			1.2(9)/0.5(9)	−2.0(9)		
α-44′biPyHI·H_2O	[010]	9.7087(2)	31.0(4)/31.6(4)	−36.2(4)	0.64(4)	175.0(1)/173.5(1)
β-44′biPyHI·H_2O	[001]	9.7150(3)	29.7(4)/29.1(4)	−32.3(3)	0.61(5)	176.1(1)/176.7(1)
44′biPyHClO$_4$·$2H_2O$	[010]	9.765(2)	22.5(7)/24.6(7)	−23.9(6)	0.68(7)	179.1(2)/178.4(2)
		9.765(2)	19.7(7)/22.1(7)	−21.7(6)	0.60(8)	178.5(2)/178.5(2)
44′biPyHBF$_4$·1/2H_2O	[110] and [1$\bar{1}$0]	9.766(2)	26.6(3)/25.9(4)	−23.9(3)	0.75(4)	176.6(1)/176.7(1)
44′biPy$_2$H$_2$SiF$_6$·5H_2O	[010]	9.762(1)	36.9(8)/25.1(9)	−31.6(8)	1	177.8(3)/179.1(3)

[a] Chain-segment length (*L*); torsion angles C3−C4−C4′−C3′ (τ_1) and C5−C4−C4′−C5′ (τ_2); intercationic torsion angle C2−N1···N1′−C2′ (τ_3); the site occupation factor for H1$^+$ (SOF H1); and intercationic angles C4−N1···N1′ (η) and N1···N1′−C4′ (η'). Pyridine rings in 44′biPyHCl·$2H_2O$ are disordered; hence, two sets of angles τ_1, τ_2, and τ_3. Two data sets for 44′biPyHClO$_4$·$2H_2O$ describe two independent cations in this structure.

dabcoHI cations and $NH^+ \cdots N$ bonds are exactly aligned along the chains (angles η and η' are exactly 180°),[4,6] and both H sites are equally favored. Likewise, the protons are nearly 50:50 disordered in the 44′biPyH*A*·*x*H_2O structures where angles η and η' are close to 180° (Table 2).

The similar structural elements of $NH^+ \cdots N$-bonded chains lead to isostructural features of the 44′biPyH*A* monosalts. Monosalts can be classified as 3-, 2-, and at least 1-dimensionally isostructural.[28] Crystals α-44′biPyHI·H_2O and 44′biPyHBr·H_2O are 3-D isostructural and crystallize in the same space group $P2_12_12_1$. They are also 3-D isostructural with the 44′biPyHCl·$2H_2O$ crystal: it has similar unit-cell parameters; however, due to the conformational disorder the space group symmetry is increased to *Pnma*.

The triclinic structure of dihydrate 44′biPyHClO_4·$2H_2O$ considerably differs from the monohydrates. In 44′biPyHClO_4·$2H_2O$ there are two independent 44′biPyH^+ cations; four independent water molecules and two independent anions form H-bonded layers along the (001) planes (Figures 1d and 2d). Despite the structural resemblance of ClO_4^- and BF_4^- anions, the crystal structure of 44′biPyHBF_4·1/2H_2O is very different than 44′biPyHClO_4·$2H_2O$. Unlike in other 44′biPyH*A*·*x*H_2O compounds, where the $NH^+ \cdots N$-bonded chains are all parallel to one of the crystal axes (Table 2), the chains in 44′biPyHBF_4·1/2H_2O run along diagonals [110] and [$1\bar{1}0$]. Another difference between 44′biPyHClO_4·$2H_2O$ and 44′biPyHBF_4·1/2H_2O is that anion ClO_4^- is ordered and BF_4^- is disordered. The disorder of the BF_4^- anion may be due to weak intermolecular interactions of the fluorine atoms, which may be also connected with the low contents of crystalline water in this structure.

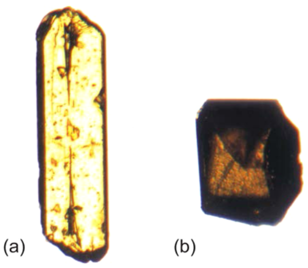

Figure 3. Crystals of the polymorphic forms of 44′biPyHI·H_2O: (a) polymorph α and (b) polymorph β.

Polymorphs of 44′biPyHI·H_2O. 44′biPyHI·H_2O polymorphs α and β can be easily distinguished by their orthorhombic and triclinic crystal habits and different colors, yellow and orange, respectively (Figure 3). These colors correspond to the conformations of cations. The larger dihedral angle between pyridine rings in α-44′biPyHI·H_2O, corresponding to a weaker conjugation of aromatic electrons across the C4−C4′ bond, which is consistent with the less intense color. In α-44′biPyHI·H_2O, water molecules and anions form zigzag chains, running between the chains of 44′biPyH^+ cations, along the [100] direction (Figure 4). The graph descriptor of this chain is $C_2^1(4)$.[29−31] The water oxygen atom forms short $CH \cdots O$ contacts to the hydrogens at pyridinium carbons C5′ and C6 (Table 3); there are also weak interactions between atoms H2′ and I1. In polymorph β the iodide ions and water molecules aggregate into planar cyclic tetramers located around the inversion centers. The graph descriptor of the cyclomer is $R_4^2(8)$. The tetramers do not interact between themselves but form the close contacts with pyridine rings (Table 3).

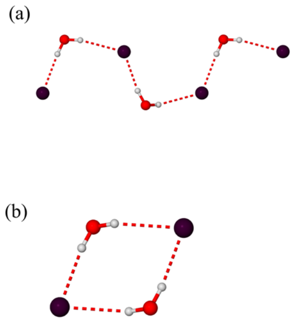

Figure 4. Iodide−water $OH \cdots I^-$ hydrogen-bonded aggregates 44′biPyHI·H_2O in (a) polymorph α and (b) polymorph β.

The $NH^+ \cdots N$ bonds (Table 4) linking the 4,4′-bipyridinium cations into linear chains are on average 2.718 Å long and about 0.104 Å shorter than those in the dabcoH*A*[6,32] and 0.115 Å shorter than in pyrazine salts.[7] In this respect, activation of proton dynamics should be the easiest in 44′biPyH*A* hydrates. The shortest $NH^+ \cdots N$ distance is in 44′biPyHBr·H_2O, where the proton is most ordered of all 44′biPyH*A*·*x*H_2O structures investigated at 296 K in this study. It suggests that the effects of the crystal environment and displacements of the H-bonded cations are more significant for the proton site than the $N^+ \cdots N$ distance. The disorder of protons in the crystal can be in principle due either to the disorder of chains or to the disorder of protons within the $NH^+ \cdots N$-bonded chains. It was confirmed by dielectric spectroscopy[2−8,18] and observation of ionic disparity in pyrazole[33] that the protons are disordered within the chains.

The mechanism of proton disorder is still being investigated: the protons can dynamically hop between their two sites, and there may be a static contribution of disproportionated 44′biPy molecules, 44′biPyH^+ cations, and 44′biPyH_2^{2+} dications, as illustrated in Figure 5. It was established that the protons are ordered in 44′biPyHBr·H_2O at 90 K,[13] which suggest that the dynamic disorder of protons is dominant in this structure. It was reported that protons are ordered in 44′biPyHClO_4 at 296 K; however, refinements of our data consistently refined to the disordered model (Table 2). Most recently we showed that the defects generated by proton disordering in $NH^+ \cdots N$ bonds in pyrazole can be segregated at the symmetry-independent sites in the structure, and in this way it can contribute to the polarization of the crystal.[33] In the 44′biPyH*A*·*x*H_2O structures, it is also possible that the proton disorder is associated with the changed polarity of the neighboring chains, or that both the disorder types, within the chains and between the chains, exist simultaneously.

4. CONCLUSIONS

It can be concluded that hydrogen-bonded 44′biPyH*A* monosalts exhibit a series of characteristic features which can be attributed to the structure and properties of 44′biPyH^+ cations (Table 5). Most importantly, they aggregate into $NH^+ \cdots N$-bonded chains, analogous to those associated with ferroelectric and relaxor properties in dabcoH*A* analogues (Table 5). At normal conditions the protons are disordered at different ratios in the $NH^+ \cdots N$ bonds of 44′biPyH*A* chains.

Several other structural features of 44′biPyH*A* salts are puzzling, particularly when referred to analogous dabcoH*A*

Table 3. Dimensions of Short Intermolecular Contacts in 44′biPyHI·H_2O Polymorphs α and β^a

D−H···*A*	D−H (Å)	H···*A* (Å)	D···*A* (Å)	D−H···*A* (deg)	symmetry code
polymorph α					
O1W−H1W···I1	1.00(1)	2.75(2)	3.656(3)	151(3)	
O1W−H2W···I1^{i}	0.99(1)	2.53(1)	3.514(2)	169(3)	(i) $1 - x, 0.5 + y, 0.5 - z$
C2′−H2′···I1^{ii}	0.93	3.09	4.003(3)	169	(ii) $0.5 - x, 2 - y, 0.5 + z$
C5′−H5′···O1W^{iii}	0.93	2.59	3.488(4)	163	(iii) $-x, -0.5 + y, 0.5 - z$
C6−H6···O1W^{iv}	0.93	2.56	3.424(4)	155	(iv) $x, -1 + y, z$
polymorph β					
O1W−H1W···I1^{v}	1.00(1)	2.74(2)	3.685(3)	158(4)	(v) $x, 1 + y, z$
O1W−H2W···I1^{vi}	1.00(1)	2.55(1)	3.549(3)	174(4)	(vi) $-x, 1 - y, 1 - z$
C2−H2···I1^{vii}	0.93	3.05	3.978(3)	177	(vii) $x, y, -1 + z$
C5−H5···O1W	0.93	2.59	3.513(4)	169	
C5′−H5′···O1W^{viii}	0.93	2.55	3.312(4)	139	(viii) $1 - x, 2 - y, 1 - z$

[a] Hydrogen bonds NH^+···N are compared in Table 4. Dimensions involving the H atoms located from the molecular geometry are listed without standard deviations.

Table 4. Dimensions of Hydrogen Bonds NH^+···N in the 44′biPy*HA* Hydrates^a

compound	N1−H1 [Å]	H1···N1′ [Å]	N1···N1′ [Å]	N1−H1···N1′ [deg]
44′biPyHBr·H_2O	0.86	1.820	2.675(4)	172
44′biPyHCl·$2H_2O$	0.984(9)	1.727(9)	2.711(3)	180(2)
α-44′biPyHI·H_2O	0.86	1.858	2.712(3)	173
β-44′biPyHI·H_2O	0.86	1.849	2.706(3)	175
44′biPyHClO_4·$2H_2O$	0.86	1.857	2.717(6)	179
	0.86	1.863	2.723(5)	179
44′biPyHBF_4·$^1/_2H_2O$	0.86	1.897	2.755(3)	176
44′biPy$_2H_2SiF_6$·$5H_2O$	0.86	1.885	2.743(3)	175

[a] Dimensions involving the protons located from molecular geometry are listed without standard deviations.

Table 5. Comparison of 44′biPy*HA*·xH_2O and dabco*HA* Structures of the Crystal Phases Stable at Ambient Conditions

44′biPy*HA*·xH_2O	at 296K and 0.1 MPa	dabco*HA*
NH^+···N-bonded chains	=	NH^+···N-bonded chains
44′biPyH^+ cations at general positions	≠	dabcoH^+ cations at special positions
A^- anions at general position	≠	A^- anions at special position
A^- anions located close to NH^+···N	=	A^- anions located close to NH^+···N
all hydrates, $x = 1/2, 1, 2$	≠	all anhydrates
all cations in twisted conformation	≠	planar N−C−C−N bridges
H^+ disordered ($A^- = Br^-, Cl^-, I^-, BF_4^-, ClO_4^-$)	=	H^+ disordered for $A^- = Br^-$ and I^-
	≠	H^+ ordered for $A^- = BF_4^-$, ClO_4^-, and ReO_4^-

salts. It is most likely due to the molecular shape that all investigated 44′biPy*HA* monosalts crystallize as hydrates, whereas all analogous dabco*HA* salts formed anhydrous crystals when crystallized in open vials in the laboratory (Table 5). In some of the 44′biPy*HA*·xH_2O salts water molecules are clearly located close to the C4−C4′ junctions of the 44′biPyH^+ cations, where some void space is available. Another striking feature of all investigated 44′biPy*HA* salts is the twisted conformation of the 44′biPy cations, while most of the known structures of 44′biPy2*HA* disalts contain planar dications only. It is apparent that at normal conditions 44′biPy*HA* salts exhibit a wider variety of crystal structures compared to dabco*HA* analogues where two isostructural classes were found, one for spherical anions $A^- = Br^-$ and I^- and another for tetrahedral anions $A^- = ClO_4^-$, BF_4^- and ReO_4^-. A manifestation of this variety among 44′biPy*HA* salts is the polymorphism of α-44′biPyHI·H_2O and β-44′biPyHI·H_2O; in analogous dabcoHI only hexagonal polymorph VI could be obtained at normal conditions, although it could be converted by heating into orthorhombic polymorph V, stable for several days at 296 K before converting back to form VI. Our study suggests that most of the specific features of 44′biPy*HA*·xH_2O salts are connected to the specific shape and conformational flexibility of the 44′biPy molecule and its cations. The disorder of protons observed in all 44′biPy*HA*·xH_2O hydrates suggests that their dielectric properties can be similar to those of dabco*HA* NH^+···N analogs.

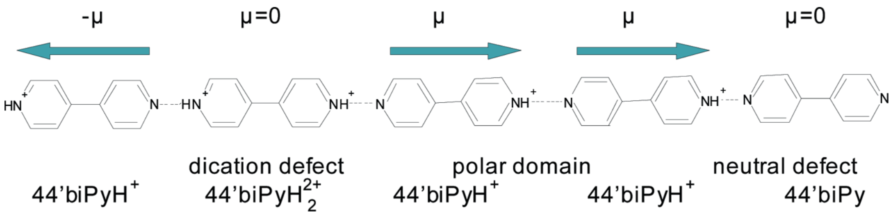

Figure 5. Chain interval of NH^+···N-bonded disproportionated 44′biPyH^+ cations, 44′biPyH_2^{2+} dications, and 44′biPy molecules. 44′biPy molecules and 44′biPyH_2^{2+} dications separate the chain fragments of opposite polarization, depending on the H^+ position in the hydrogen bonds.

ASSOCIATED CONTENT

Supporting Information

Details of syntheses; melting points of synthesized monosalts and disalts; crystal data for 4,4′-bipyridinium monosalt hydrates; atomic coordinates and U_{eq} parameters, anisotropic displacement parameters, bond lengths and angles; crystallographic data (CCDC 936066−936072) in CIF format. This material is available free of charge via the Internet at http://pubs.acs.org.

AUTHOR INFORMATION

Corresponding Author

*E-mail: katran@amu.edu.pl.

Notes

The authors declare no competing financial interest.

ACKNOWLEDGMENTS

This study was supported by the Polish Ministry of Science and Higher Education, project N N204 86838.

REFERENCES

(1) Horiuchi, S.; Tokunaga, Y.; Giovannetti, G.; Picozzi, S.; Itoh, H.; Shimano, R.; Kumai, R.; Tokura, Y. *Nature* **2010**, *463*, 789−792.

(2) Katrusiak, A.; Szafrański, M. *Phys. Rev. Lett.* **1999**, *82*, 576−579.

(3) Szafrański, M.; Katrusiak, A.; McIntyre, G. J. *Phys. Rev. Lett.* **2002**, *89*, 215507−215510.

(4) Szafrański, M.; Katrusiak, A. *J. Phys. Chem. B* **2004**, *108*, 15709−15713.

(5) Szafrański, M.; Katrusiak, A. *J. Phys. Chem. B* **2008**, *112*, 6779−6785.

(6) Katrusiak, A.; Ratajczak-Sitarz, M.; Grech, E. *J. Mol. Struct.* **1999**, *474*, 135−141.

(7) Katrusiak, A.; Szafrański, M. *J. Am. Chem. Soc.* **2006**, *128*, 15775−15785.

(8) Szafrański, M.; Katrusiak, A.; McIntyre, G. J. *Cryst. Growth Des.* **2010**, *10*, 4334−4338.

(9) Dega-Szafran, Z. *Bull. Acad. Polon. Sci., Ser. Sci. Chim.* **1979**, *27*, 267−272.

(10) Iyere, P. A.; Kayren, I. J.; Cordes, A. W.; Eagle, C. T.; Nile, T. A.; Schimek, G. I.; Pennington, W. T. *Cryst. Eng.* **1998**, *1*, 159−167.

(11) Iyere, P. A.; Boadi, W. Y.; Brooks, R. S.; Atwood, D.; Parkin, S. *Acta Crystallogr., Sect. B* **2003**, *59*, 664−669.

(12) Ng, S. W. *Acta Crystallogr., Sect. C* **1999**, *55*, 2105−2107.

(13) Iyere, P. A.; Boadi, W. Y.; Brooks, R. S.; Atwood, D.; Parkin, S. *Acta Crystallogr., Sect. E* **2002**, *58*, o825−o827.

(14) Zhang, J.-Y.; Cheng, A.-L.; Gao, E.-Q. *J. Chem. Crystallogr.* **2008**, *38*, 351−355.

(15) Sheldrick, G. M. *Acta Crystallogr., Sect. A* **2008**, *64*, 112−122.

(16) Olejniczak, A.; Katrusiak, A. *Cryst. Growth Des.* **2011**, *11*, 2250−2256.

(17) Dziubek, K. F.; Katrusiak, A. *J. Phys. Chem. B* **2004**, *108*, 19089−19092.

(18) Olejniczak, A.; Katrusiak, A.; Szafrański, M. *Cryst. Growth Des.* **2010**, *10*, 3537−3546.

(19) Bondi, A. *J. Phys. Chem.* **1964**, *68*, 441−452.

(20) Kitaigorodsky, A. I. *Acta Phys. Chim. USSR* **1946**, *21*, 575−576.

(21) Toudic, B.; Gallier, J.; Rivet, P.; Cailleau, H. *Solid State Commun.* **1983**, *47*, 291−195.

(22) Natkaniec, I.; Bielushkin, A. V.; Wasiutyński, T. *Phys. Status Solidi B* **1981**, *105*, 413−423.

(23) Dhar, J. *Indian J. Phys.* **1932**, *7*, 43−60.

(24) Bastiansen, O. *Acta Chem. Scand.* **1949**, *3*, 408−414.

(25) Cruickshank, D. W. J. *Acta Crystallogr.* **1956**, *9*, 1005−1009.

(26) Baudour, J. L. *Crystallogr. Rev.* **1996**, *5*, 227−264.

(27) Katrusiak, A. *J. Mol. Struct.* **1999**, *474*, 125−133.

(28) Fábián, L.; Kálmán, A. *Acta Crystallogr., Sect. B* **2004**, *58*, 547−558.

(29) Etter, M. C. *Acc. Chem. Res.* **1990**, *23*, 120−126.

(30) Etter, M. C.; McDonald, J. C.; Bernstein, J. *Acta Crystallogr., Sect. B* **1990**, *46*, 256−262.

(31) Grell, J.; Bernstein, J.; Tinhofer, G. *Acta Crystallogr., Sect. B* **1999**, *55*, 1030−1043.

(32) Katrusiak, A. *J. Mol. Struct.* **2000**, *552*, 159−164.

(33) Sikora, M.; Katrusiak, A. *J. Phys. Chem. C* **2013**, *117*, 10661−10668.